



## P-type Ca doped SrCu<sub>2</sub>O<sub>2</sub> thin film: Synthesis, optical property and photovoltaic application

Yiping Zhao<sup>a,b</sup>, Weiwei Dong<sup>a,b,\*</sup>, Xiaodong Fang<sup>a,b</sup>, Yikai Zhou<sup>c</sup>, Gang Meng<sup>a,b</sup>, Ruhua Tao<sup>a,b</sup>, Zanhong Deng<sup>a,b</sup>, Shu Zhou<sup>a</sup>, Songyuan Dai<sup>b</sup>

<sup>a</sup> Anhui Provincial Key Laboratory of Photonic Devices and Materials, Anhui Institute of Optics and Fine Mechanics, Chinese Academy of Sciences, Hefei 230031, China

<sup>b</sup> Key Laboratory of New Thin Film Solar Cells, Institute of Plasma Physics, Chinese Academy of Sciences, Hefei 230031, China

<sup>c</sup> The Institute of Scientific and Industrial Research, Osaka University, Osaka 5670047, Japan

### ARTICLE INFO

#### Article history:

Received 13 December 2010

Received in revised form

21 September 2011

Accepted 22 September 2011

Available online 29 September 2011

#### Keywords:

Transparent conducting oxide

P-type

Heterojunction

Thin film solar cell

### ABSTRACT

P-type transparent conducting oxide Sr<sub>0.9</sub>Ca<sub>0.1</sub>Cu<sub>2</sub>O<sub>2</sub> (SCCO) films were prepared by pulsed laser deposition (PLD) technique on glass and n-Si (100) substrates. Some critical experiment factors were investigated, and it was found that well-crystallized, single phase SCCO films could be obtained with the substrate temperature higher than 350 °C, and the crystallinity was improved with the increase of laser energy fluence. Sr<sub>0.9</sub>Ca<sub>0.1</sub>Cu<sub>2</sub>O<sub>2</sub>/n-Si (SCCO/n-Si) heterojunction and prototype thin film solar cell were demonstrated respectively. Diode characteristic in the current–voltage response was observed and the ideality factor (*n*) of the diode was 3.7. The obtained *n* value is larger than unity due to structural imperfections of the layer and interface states. A prototype thin film solar cell with the best solar cell performance exhibits an open-circuit voltage (*V*<sub>oc</sub>) of 140 mV and a short-circuit current density (*J*<sub>sc</sub>) of 0.072 mA/cm<sup>2</sup> under irradiation of AM1.5 and 100 mW/cm<sup>2</sup>.

© 2011 Elsevier B.V. All rights reserved.

## 1. Introduction

Photovoltaic power generation has attracted more attention due to energy crisis and environment pollution. In order to promote the use of photovoltaic devices, it is necessary to develop solar cells with low cost, high efficiency and less environmental damaging. A variety of materials could be used for the preparation of heterojunction solar cells [1–3]. Thin film solar cells is a promising approach and offer many choices in terms of materials and device designing [4–7]. A variety of substrates can be used for deposition of different layers. Among all, silicon is a widely used substrate because it is cheap, conductive and easy to cleave, so it is valuable to grow different thin films on Si substrate.

With excellent chemical, physical and optoelectronic properties, transparent conductive oxides (TCOs) have many advanced technology applications, such as photovoltaic solar cells, transparent electrodes and other optoelectronic devices [8,9]. Some thin film solar cells have been obtained by employing TCO films on Si substrates, such as ITO, ZnO, ZnO: Al, CdO, and relative high

conversion efficiencies have been obtained by employing ITO films on Si substrate [10–13].

As one of the most important TCO materials, p-type transparent conducting ternary Cu (I) oxides (CuAlO<sub>2</sub>, CuCrO<sub>2</sub>, CuGaO<sub>2</sub>, CuYO<sub>2</sub>, SrCu<sub>2</sub>O<sub>2</sub>, etc.) have attracted widespread interests, and different techniques have been used for the preparation of this kind of TCO thin films [14–21]. The ternary oxide SrCu<sub>2</sub>O<sub>2</sub> has a direct band gap of 3.3 eV in combination with non-toxicity and relatively low deposition temperature [22]. There are many reports on fabrication and optoelectronic applications of Sr<sub>1-x</sub>M<sub>x</sub>Cu<sub>2</sub>O<sub>2</sub> (M = Ca, K) films [23–29]. To our knowledge, SrCu<sub>2</sub>O<sub>2</sub>/Si heterojunctions have been obtained by PLD with different substrate temperatures and laser wavelengths [27,28], but Sr<sub>0.9</sub>Ca<sub>0.1</sub>Cu<sub>2</sub>O<sub>2</sub> (SCCO)/Si heterojunction and its photovoltaic performance have not been investigated. In this study, SCCO films were prepared on glass and n-Si (100) substrates and the electrical property of the SCCO/n-Si heterojunction was analyzed by current–voltage technique at room temperature. The photovoltaic performance of the SCCO/n-Si heterojunction was reported for the first time.

## 2. Experimental details

Ca doped SrCu<sub>2</sub>O<sub>2</sub> polycrystalline ceramic target was synthesized by sintering fully mixed powder of Cu<sub>2</sub>O (99.5% purity), SrCO<sub>3</sub> (99.9% purity) and CaCO<sub>3</sub> (99% purity) (with molar ratio of 1:0.9:0.1) at 950 °C for 40 h in N<sub>2</sub> flow. The Sr<sub>0.9</sub>Ca<sub>0.1</sub>Cu<sub>2</sub>O<sub>2</sub> (SCCO) thin films were deposited by PLD on glass and n-type Si (100) wafer substrates. The resistivity and carrier concentration of n-Si (100) substrate were about 8–15 Ω cm and 10<sup>15</sup> cm<sup>-3</sup>, respectively. Prior to growth, glass and n-type

\* Corresponding author at: Anhui Institute of Optics and Fine Mechanics, Chinese Academy of Sciences, Hefei 230031, China. Tel.: +86 551 5593508; fax: +86 551 5593527.

E-mail address: [wwdong@aiofm.ac.cn](mailto:wwdong@aiofm.ac.cn) (W. Dong).

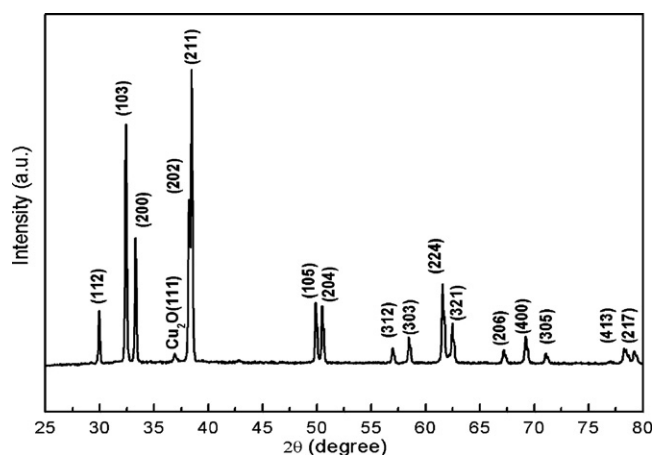


Fig. 1. XRD pattern of SCCO target.

Si (1 00) wafer were cleaned by ultrasonication in acetone, ethanol and de-ionized water, respectively, finally dried by nitrogen flow. The native oxide on the surface of silicon substrate was not removed using HF solution. The base pressure of PLD chamber was  $10^{-5}$  Pa, and the laser employed was a KrF excimer laser ( $\lambda = 248$  nm) with a repetition rate of 5 Hz. The beam was incident on a rotating target at an angle of  $45^\circ$  with respect to target normal. Oxygen gas was introduced into the deposition chamber and working pressure was controlled at  $1 \times 10^{-2}$  Pa. The substrate temperatures were kept at  $350^\circ\text{C}$ ,  $420^\circ\text{C}$ ,  $480^\circ\text{C}$  and  $540^\circ\text{C}$  and the duration of deposition was 0.5 h. The energy fluence used to deposited SCCO films on glass substrate was 110 mJ/pulse. SCCO films were also deposited on Si wafer with the same deposition parameters like those deposited on glass but the energy fluences were 110 mJ/pulse and 150 mJ/pulse. After the deposition, the films were cooled to room temperature under the same oxygen pressure.

The crystal structure of the film was investigated using Philips X'pert PRO X-ray diffractometer (XRD) with a  $\text{CuK}\alpha$  source. Surface morphology, thickness of the films and elemental analysis were studied using FEI Sirion 200 type model scanning electron microscope (FESEM) and energy dispersive spectroscopy (EDS), respectively. Transmittance of the SCCO films deposited on glass substrate was measured in the spectral region of 200–1200 nm using a Cary-5E UV-VIS spectrophotometer. Ohmic contacts were made on the SCCO film and back surface of silicon substrate by depositing In electrodes. The resistivity of all the films was large, so the standard two-probe technique was used to measure electrical resistivity, and the van-der-Pauw four-point method was applied to measure carrier density by LakeShore-775 Hall Measurement System. The current–voltage characteristics of the diode in the dark was performed using a Keithley model 2400 digital sourcemeter and the power output was measured using a solar simulator with AM1.5 and a power density of  $100 \text{ mW}/\text{cm}^2$ .

### 3. Results and discussion

The phase of as-sintered Ca doped  $\text{SrCu}_2\text{O}_2$  target was examined by XRD. As Fig. 1 shows, the diffraction pattern can be well-indexed to tetragonal phase, belonging to  $I4_1/amd$  space group (JCPDS card no: 48-1514) except a small impurity diffraction peak at  $36.78^\circ$  which arise from unreacted  $\text{Cu}_2\text{O}$  (JCPDS card no: 01-1142).

In order to investigate optical and electrical properties of SCCO thin film, SCCO films were prepared on non-conducting glass substrate. It is well believed that PLD is a powerful thin film deposition technique, and the crystallinity, electrical property and optical property of metal oxide thin films could be tuned by adjusting experiment parameters, such as substrate temperature and oxygen pressure. In our experiments, the film synthesized under oxygen pressure of  $1 \times 10^{-2}$  Pa has the highest transmittance in visible range, so all the other SCCO films were prepared under this oxygen pressure. The substrate temperatures were kept at  $350^\circ\text{C}$ ,  $420^\circ\text{C}$ ,  $480^\circ\text{C}$  and  $540^\circ\text{C}$ , and it is found that all the films are polycrystalline which is similar with the results of other groups [29,30]. Fig. 2 gives the diffraction pattern of SCCO film deposited at  $350^\circ\text{C}$ . All the diffraction peaks can be indexed as  $\text{SrCu}_2\text{O}_2$  (JCPDS card no: 48-1514). Raising the substrate temperature gives the improvement of crystallinity of the films without new phase

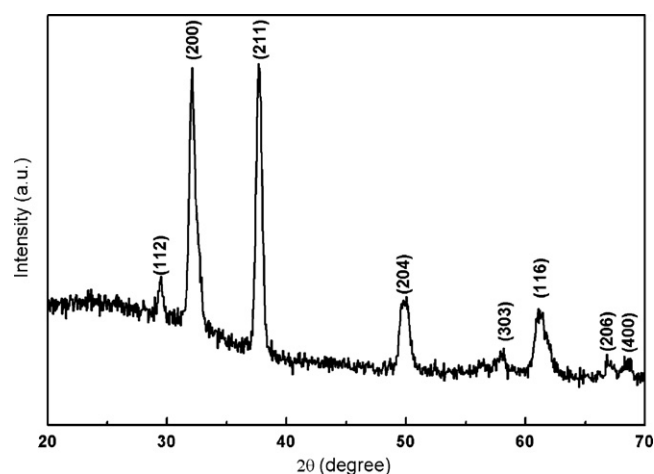


Fig. 2. XRD pattern of SCCO film prepared on glass substrate with substrate temperature of  $350^\circ\text{C}$ .

appearing (other XRD patterns are not shown here). Fig. 3 depicts the optical transmittance spectrum of this SCCO film. It exhibits  $\sim 70\%$  optical transmission in visible region (400–800 nm). The optical band gap was calculated with direct transition relationship  $(\alpha h\nu) = B(h\nu - E_g)^{1/2}$  (where  $h\nu$  is the photon energy,  $\alpha$  is absorption coefficient,  $E_g$  is optical band gap and  $B$  is a constant). The obtained  $E_g$  value is about 3.3 eV and this value is in agreement with the literature [35]. All the SCCO films are p-type obtained by Hall measurement, the resistivity and carrier density are almost in  $10^3 \Omega \text{ cm}$  and  $10^{16} \text{ cm}^{-3}$ , respectively. Here, only the electrical resistivity, carrier density, Hall mobility, Hall coefficient of the sample deposited at  $540^\circ\text{C}$  are given and they are  $1.03 \times 10^3 \Omega \text{ cm}$ ,  $1.6 \times 10^{16} \text{ cm}^{-3}$ ,  $0.38 \text{ cm}^2 \text{ V}^{-1} \text{ s}^{-1}$  and  $389 \text{ cm}^3/\text{C}$ , respectively.

For the fabrication of p-SCCO/n-Si heterojunctions, SCCO films were deposited on pieces of Si wafer under the similar experiment conditions like depositing SCCO films on glass substrate. Fig. 4(a) and (b) shows the X-ray diffraction patterns of SCCO films on Si substrate with the substrate temperatures kept at  $480^\circ\text{C}$  and  $540^\circ\text{C}$ . Raising the substrate temperature would improve the crystallinity as shown in Fig. 4. On the other hand, when the substrate temperature is kept at  $540^\circ\text{C}$ , raising the laser energy from 110 mJ/pulse to 150 mJ/pulse will greatly improve the crystallinity of SCCO films as it can be seen in Fig. 5.

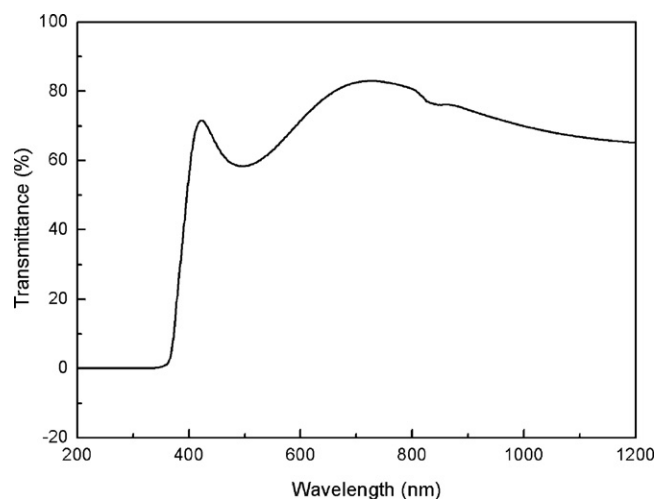


Fig. 3. Optical transmittance spectrum of SCCO film on glass substrate with substrate temperature of  $350^\circ\text{C}$ .

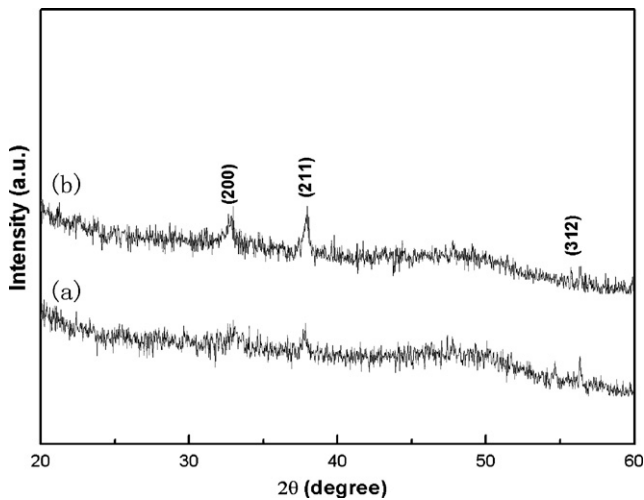


Fig. 4. XRD patterns of SCCO film on Si substrate with laser energy of 110 mJ/pulse and substrate temperatures kept at (a) 480 °C and (b) 540 °C.

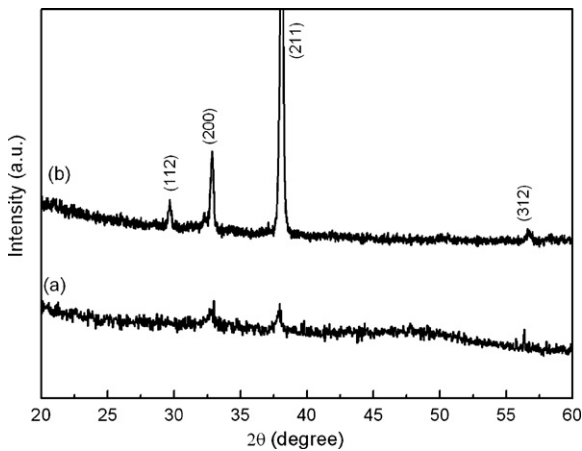


Fig. 5. XRD patterns of SCCO film on Si substrate with substrate temperatures kept at 540 °C and laser fluence of (a) 110 mJ/pulse and (b) 150 mJ/pulse.

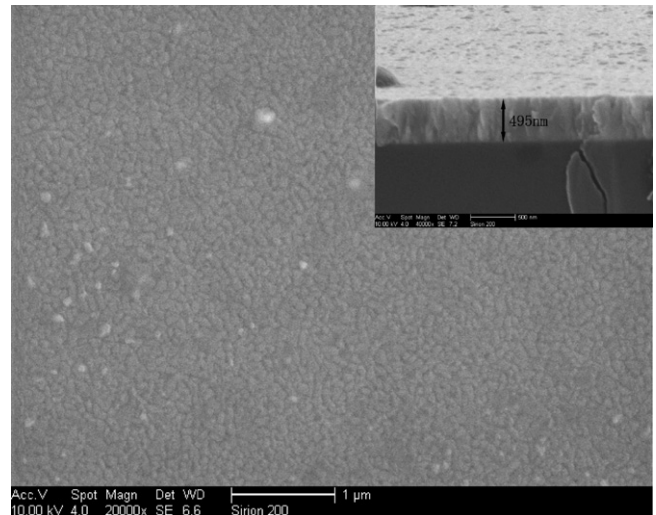


Fig. 6. SEM images of SCCO film deposited on Si substrate with laser energy of 150 mJ/pulse and substrate temperature of 540 °C. (The insert is cross-sectional FESEM of SCCO film.)

The surface morphology and cross-sectional FESEM images of the SCCO film on Si substrate with the best crystallinity are shown in Fig. 6. The surface is dense and smooth and the thickness is about 495 nm as it can be seen in the insert of Fig. 6. The EDS spectrum of the SCCO film on Si substrate is presented in Fig. 7. Only O, Ca, Cu and Sr signals are detected. The EDS results confirm that Ca is in the structure of the  $\text{SrCu}_2\text{O}_2$  films and the atomic ratio of Sr:Ca:Cu:O is about 0.9:0.1:2:2.5.

It has been shown in previous investigation that the p- $\text{SrCu}_2\text{O}_2$ /n-Si heterojunction with low temperature (300 °C) deposited  $\text{SrCu}_2\text{O}_2$  has better p/n junction properties than that with high temperature (500 °C) deposited  $\text{SrCu}_2\text{O}_2$  films because non-stoichiometric  $\text{SrCu}_2\text{O}_3$  phase appeared in high substrate temperature [27]. But in our experiments, we found that  $\text{SrCu}_2\text{O}_3$  phase could not be detected in the SCCO film deposited with substrate temperature of 540 °C. All the SCCO/n-Si heterojunctions have obvious rectifying behavior though the crystallinity of the SCCO films deposited at low substrate temperature is very poor. On the other

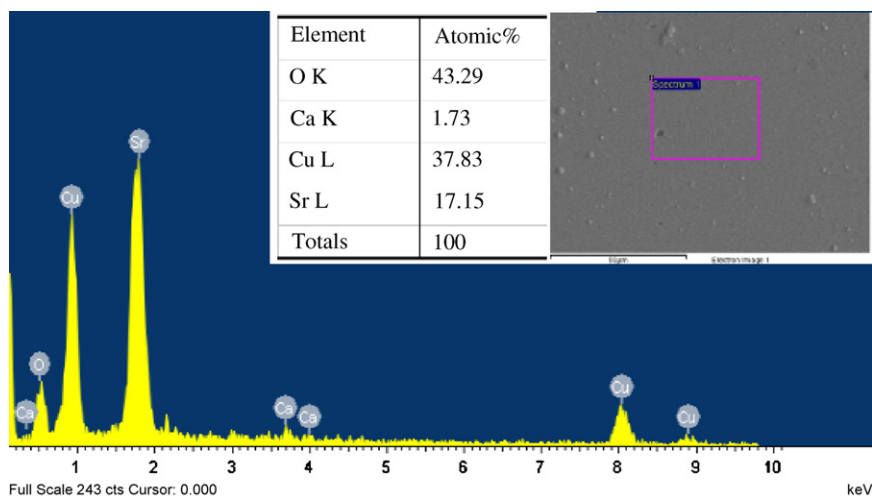
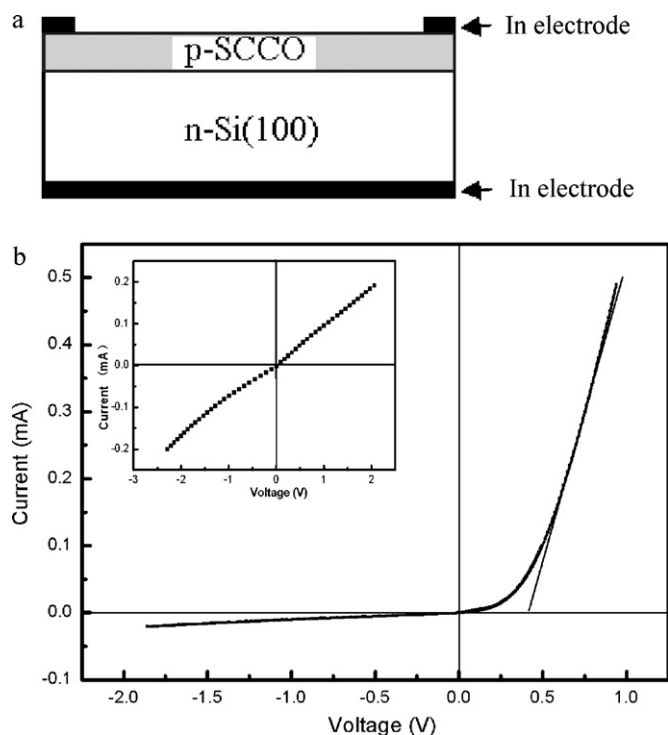


Fig. 7. Elemental analysis of the SCCO film deposited on Si substrate with laser energy of 150 mJ/pulse and substrate temperature of 540 °C. The insert is SEM image of the region analyzed.



**Fig. 8.** (a) The diode geometry of SCCO/n-Si heterojunction. (b) Current–voltage characteristics of SCCO/n-Si heterojunction. The insert shows the  $I$ – $V$  curve of In contacts on p-SCCO film.

hand, the rectifying behavior of SCCO/n-Si heterostructure with high laser energy fluence deposited SCCO films was improved greatly. It is mainly related to the improved crystallinity quality of SCCO films as it can be seen in Fig. 5. Some other reasons may also exist, such as better interface between SCCO films and Si substrate. Fig. 8(a) and (b) shows the diode geometry and  $I$ – $V$  characteristics of SCCO/n-Si heterojunction with laser energy fluence of 150 mJ/pulse and the insert of Fig. 8 (b) is the  $I$ – $V$  curve of In contacts on p-SCCO film. The contact on the SCCO exhibits a characteristic without rectifying behavior of Schottky contacts and this indicate that Ohmic contacts are formed between In electrodes and SCCO film.

From Fig. 8(b), the turn-on voltage is 0.4 V and the leakage current at  $-1.86$  V is 20  $\mu$ A. The leakage current in the reverse bias region mainly come from large lattice mismatch and the polycrystalline structure of SCCO film will induce structural imperfections existed at grain boundaries and interface. Therefore, the efficiency is deteriorated by these defects [31]. The  $I$ – $V$  characteristics of the diode can be analyzed by the following relation,

$$I = I_S e^{qV/nkT} - 1$$

where  $V$  is the applied voltage,  $n$  is the ideality factor,  $k$  is the Boltzmann's constant,  $T$  is temperature and  $I_S$  is reverse saturation current. The ideality factor of the diode was determined from the slope of the linear region of forward bias of Fig. 8(b) and it was found to be 3.7. The ideality factor of standard diode is between 1 and 2, but the obtained ideality factor of the SCCO/n-Si was higher than unity. A value greater than 2 for  $n$  indicates that the diode is not an ideal one. Most of the reported oxide semiconductors deposited on Si exhibit diode characteristics which diverge from theoretical calculations [32]. This is probably due to presence of structural imperfections of the layers and interface states and/or presence of an insulating layer at the interface. Since no standard cleaning was applied, a thin insulating layer is formed at the interface modifying the junction properties [33].

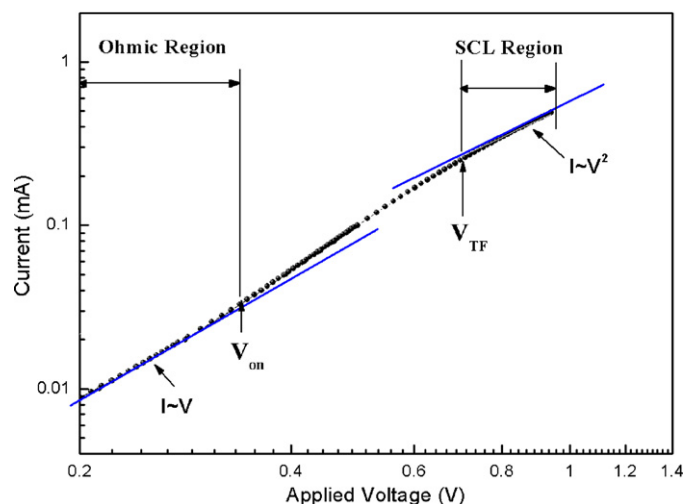


**Fig. 9.** The log  $I$ –log  $V$  plot of the SCCO/n-Si heterojunction at room temperature.

As the carrier concentration of the n-Si is lower than that of the SCCO film, the depletion space charge region is mainly located at Si side. Because of the lack of the electron affinity value of SCCO material, the valence band offset and conduction band offset cannot be obtained at this moment. It can only be suggested that as the SCCO side is under forward bias, the band barrier will decrease and carrier flow will enhance. The subsequent recombination at the depletion region would give rise to forward bias current flow. As the forward bias is large enough, the barrier would be negligible. On the other hand, a thin native oxide of insulator layer exists at the interface, it would block the collection of carriers generated at the n-Si, and it would also cause large current leakage located at the junction interface of the heterojunction [34].

In order to investigate operative mechanisms of the SCCO/n-Si heterojunction, the power law fit of  $I$ – $V$  characteristics of the heterojunction is shown in Fig. 9. When the forward bias is below 0.33 V,  $I$ – $V$  indicated Ohmic conduction prevalence. In the high bias voltage which ranges from 0.7 to 1 V,  $I$ – $V^2$ , corresponding to a shallow trap square-law region, which is a classical characteristic of space charge limited current (SCLC). Space charge limited current conduction is typically observed in wide band gap semiconductors [35–38]. Lampert and Mark have developed the single carrier SCLC model with a trap present above the Fermi level [39]. As the applied voltage is lower than the onset voltage for deviating from Ohmic behavior ( $V < V_{on}$  as shown in Fig. 9), the thermally generated carrier density dominates over the injected carrier density and the carrier transit time is larger than the dielectric relaxation time. The injected carrier would thus undergo dielectric relaxation to maintain the charge neutrality rather than transport across the sample. In this region, the traps are not completely filled. As the applied voltage is larger than  $V_{on}$ , the carrier transit time is smaller than the dielectric relaxation time and the injected carrier dominates over the thermally generated carrier. The increase of the applied voltage also shifts the quasi-Fermi level towards the conduction band and the effect would be the filling up of the trap at the energy level of  $E_c - E_t$  (where  $E_c$  is conduction band energy and  $E_t$  is trap energy), the trap filling region is  $V_{on} < V < V_{TFL}$  as shown in Fig. 9. As the applied voltage further increases to the extent that all the traps are filled ( $V > V_{TFL}$  in Fig. 9), the conduction would become space charge limited and the current follows the dependence of  $J = (9/8)\epsilon\mu V^2/d^3$  (where  $d$  is the thickness of the active region).

Finally, we fabricated SCCO/n-Si heterojunction as a prototype solar cell with a window area of 0.25 cm<sup>2</sup> without any surface protection or anti-reflection coating. The typical  $I$ – $V$  characteristic curve under sunlight illumination is shown in Fig. 10. The

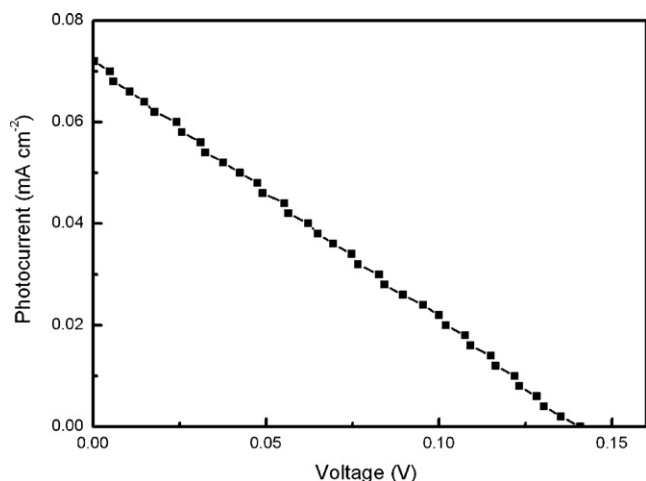


**Fig. 10.** Current–voltage characteristics of SCCO/n-Si prototype thin film solar cell under AM1.5 solar simulator illumination.

open-circuit voltage ( $V_{oc}$ ) is 140 mV and short-circuit current density ( $J_{sc}$ ) is 0.072 mA/cm<sup>2</sup> under 100 mW/cm<sup>2</sup> sunlight illumination. It is observed from Fig. 3 that the SCCO films is transparent ( $T > 70\%$ ) in visible region, therefore, most of the visible light passes through the SCCO layer and is absorbed primarily in the underlying n-Si, generating electron–hole pairs which is responsible for the observed photocurrent. Because the obtained SCCO film is polycrystalline and there is a native oxide layer in the interface, many defects exist in the interface and grain boundary which would act as carrier recombination center and depress the overall photovoltaic performance. On the other hand, both SCCO film and Si wafer have low carrier density, it will result in low value of  $V_{oc}$  [40]. The low photo-electric conversion efficiency might due to poor collection efficiency, which is probably due to recombination losses in the bulk as well as in the interface region. The poor collection efficiency probably arises because of (i) the lattice mismatch between SCC and Si layers, (ii) the high resistivity of the absorber layer, leading to increase in series resistance and decrease in fill factor. Further work is needed to improve the interface state and increase its photovoltaic performance.

#### 4. Conclusions

Polycrystalline Ca doped SrCu<sub>2</sub>O<sub>2</sub> films were grown on glass and n-type Si (1 0 0) substrates by PLD. The films deposited on glass substrate have 70% transmittance in visible region. Diode characteristic was observed in Sr<sub>0.9</sub>Ca<sub>0.1</sub>Cu<sub>2</sub>O<sub>2</sub>/n-Si (SCCO/n-Si) heterojunction and the operative mechanism of the SCCO/n-Si heterojunction was investigated. A prototype thin-film p-SCCO/n-Si heterojunction solar cell showed a maximum open-circuit voltage ( $V_{oc}$ ) of 140 mV and a short-circuit current density ( $J_{sc}$ ) of 0.072 mA/cm<sup>2</sup> under sunlight of AM1.5. This is the first reported photovoltaic result using wide gap p-type TCO material combined with n-type silicon substrate until now.

#### Acknowledgements

This work was supported by the Knowledge Innovation Program of the Chinese Academy of Sciences, Key Laboratory of

Functional Crystals and Laser Technology, Anhui Provincial International Science and Technology Cooperation Program (Grant No. 10080703021), National Basic Research Program of China (Grant No. 2011CBA00700), and the National High Technology Research and Development Program of China (Grant No. 2011AA050527).

#### References

- [1] S.H. Park, A. Roy, S. Beaupré, S. Cho, N. Coates, J.S. Moon, D. Moses, M. Leclerc, K. Lee, A.J. Heeger, *Nat. Photonics* 3 (2009) 297–302.
- [2] G.K. Mor, O.K. Varghese, Paulose S.M., K. Shankar, C.A. Grimes, *Sol. Energy Mater. Sol. Cells* 90 (2006) 2011–2075.
- [3] B. Johann, R. Punniamoorthy, N. Jenny, *J. Mater. Chem.* 17 (2007) 3141–3153.
- [4] F. Vasilis, *Renew. Sustain. Energy Rev.* 13 (2009) 2746–2750.
- [5] G. Aberle Armin, *Thin Solid Films* 517 (2009) 4706–4710.
- [6] S. Buecheler, D. Corica, D. Guettler, A. Chirila, R. Verma, U. Müller, T.P. Niesen, J. Palm, A.N. Tiwari, *Thin Solid Films* 517 (2009) 2312–2315.
- [7] S.M. Wong, H.Y. Yu, J.S. Li, G. Zhang, P. Lo, D.L. Kwong, *IEEE Electron Devices Lett.* 31 (2010) 335–337.
- [8] F. Elvira, G. David, H. Hideo, D.C. Paine, *Mater. Res. Bull.* 32 (2007) 242–247.
- [9] T. Soederstroem, F.-J. Haug, X. Niquille, *Prog. Photovoltaics* 17 (2009) 165–176.
- [10] W. Zhang, Q. Meng, B. Lin, Z. Fu, *Sol. Energy Mater. Sol. Cells* 92 (2008) 949–952.
- [11] O. Lupan, S. Shishiyuan, V. Ursaki, H. Khallaf, L. Chow, T. Shishiyuan, V. Sontea, E. Monaico, S. Railean, *Sol. Energy Mater. Sol. Cells* 93 (2009) 1417–1422.
- [12] F. Yakuphanoglu, M. Caglar, Y. Caglar, S. Ilcan, *J. Alloys Compd.* 506 (2010) 188–193.
- [13] G.G. Untila, T.N. Kost, A.B. Chebotareva, M.B. Zaks, A.M. Sitnikov, O.I. Solodukha, *Semiconductors* 42 (2008) 406–413.
- [14] Z. Deng, X. Fang, R. Tao, W. Dong, S. Zhou, G. Meng, J. Shao, *J. Alloys Compd.* 509 (2011) 5300–5304.
- [15] Y. Wang, Y. Gu, T. Wang, W. Shi, *J. Alloys Compd.* 509 (2011) 5897–5902.
- [16] D. Oh, Y.S. No, S.Y. Kim, W.J. Cho, K.D. Kwack, T.W. Kim, *J. Alloys Compd.* 509 (2011) 2176–2179.
- [17] H.F. Jiang, X.B. Zhu, H.C. Lei, G. Li, Z.R. Yang, W.H. Song, J.M. Dai, Y.P. Sun, Y.K. Fu, *J. Alloys Compd.* 509 (2011) 1768–1773.
- [18] M. Amami, S. Smari, K. Tayeb, P. Strobel, A. Ben Salah, *Mater. Chem. Phys.* 128 (2011) 298–302.
- [19] M. Amami, F. Jlael, P. Strobel, A. Ben Salah, *Mater. Res. Bull.* 46 (2011) 1729–1733.
- [20] T. Sugimoto, A. Yanagawa, T. Hashimoto, *Thermochim. Acta*, doi:10.1016/j.tca.2011.03.002.
- [21] N. Michael, *Thin Solid Films* 516 (2008) 8130–8135.
- [22] A. Kudo, H. Yanagi, H. Hosono, H. Kawazoe, *Appl. Phys. Lett.* 73 (1998) 220–222.
- [23] H. Ohta, K. Kawamura, M. Orita, N. Sarukura, M. Hirano, H. Hosono, *Electron. Lett.* 36 (2000) 984–985.
- [24] H. Ohta, K. Kawamura, M. Orita, M. Hirano, N. Sarukura, H. Hosono, *Appl. Phys. Lett.* 77 (2000) 475–477.
- [25] H. Ohta, M. Orita, M. Hirano, *J. Appl. Phys.* 89 (2001) 5720–5725.
- [26] H. Hosono, H. Ohta, K. Hayashi, M. Orita, M. Hirano, *J. Cryst. Growth* 237–239 (2002) 496–502.
- [27] E.L. Papadopoulou, M. Varda, A. Pennos, M. Kaloudis, M. Kayambaki, M. Androulidaki, K. Tsagaraki, Z. Viskadourakis, O. Durand, G. Huyberegts, E. Aperathitis, *Thin Solid Films* 516 (2008) 8154–8158.
- [28] D. Louloudakis, M. Varda, E.L. Papadopoulou, M. Kayambaki, K. Tsagaraki, V. Kambalafka, M. Modreanu, G. Huyberegts, E. Aperathitis, *Phys. Status Solidi A* 207 (2010) 1726–1730.
- [29] S. Sheng, G. Fang, C. Li, Z. Chen, S. Ma, L. Fang, X. Zhao, *Semicond. Sci. Technol.* 21 (2006) 586–590.
- [30] D.S. Ginley, C. Bright, *Mater. Res. Bull.* 25 (2000) 15–18.
- [31] A. Kudo, H. Yanagi, K. Ueda, H. Hosono, H. Kawazoe, Y. Yano, *Appl. Phys. Lett.* 75 (1999) 2851–2853.
- [32] A.N. Banerjee, K.K. Chattopadhyay, *Prog. Cryst. Growth Charact. Mater.* 50 (2005) 52–105.
- [33] S. Mridha, D. Basak, *J. Appl. Phys.* 101 (2007), 083102-1–083102-5.
- [34] Y.S. Choi, J.Y. Lee, W.H. Choi, H.W. Yeom, S. Im, *Jpn. J. Appl. Phys.* 41 (2002) 7357–7358.
- [35] O.J. Marsh, C.R. Viswanathan, *J. Appl. Phys.* 38 (1967) 3135–3144.
- [36] S. Tehrani, J.S. Kim, L.L. Hench, C.M. Van Vleet, G. Bosman, *J. Appl. Phys.* 58 (1985) 1562–1570.
- [37] H.P. Hall, M.A. Awaah, K. Das, *Phys. Status Solidi A* 201 (2004) 522–528.
- [38] R.L. Hoffman, J.F. Wagner, M.K. Jayaraj, J. Tate, *J. Appl. Phys.* 90 (2001) 5763–5767.
- [39] M.A. Lampert, P. Mark, *Current Injection in Solids*, Academic, New York, 1970.
- [40] J. Sites, J. Pan, *Thin Solid Films* 515 (2007) 6099–6102.